Multi-Scale Simulation of Radiation Effects in Electronic Devices

Ronald D. Schrimpf, *Fellow, IEEE*, Kevin M. Warren, Dennis R. Ball, Robert A. Weller, *Senior Member, IEEE*, Robert A. Reed, *Member, IEEE*, Daniel M. Fleetwood, *Fellow, IEEE*, Lloyd W. Massengill, *Fellow, IEEE*, Marcus H. Mendenhall, Sergey. N. Rashkeev, Sokrates T. Pantelides, and Michael A. Alles, *Member, IEEE*

***Abstract*—As integrated circuits become smaller and more complex, it has become increasingly difficult to simulate their responses to radiation. The distance and time scales of relevance extend over orders of magnitude, requiring a multi-scale, hierarchical simulation approach. This paper demonstrates the use of multi-scale simulations to examine two radiation-related problems: enhanced low-dose-rate sensitivity (ELDRS) in bipolar transistors and single-event effects (SEE) in CMOS integrated circuits. Examples are included that demonstrate how information can be passed from simulation tools operating at one level of abstraction to those operating at higher levels, while maintaining accuracy and gaining insight.**

***Index Terms*—Integrated circuits, multi-scale simulation, radiation, single-event effects, total ionizing dose.**

I. Introduction

CHANGES in microelectronic materials and device structures have resulted in very significant changes to integrated-circuit technologies in recent years. These changes have the potential to affect radiation hardness in dramatic and unexpected ways. Energy deposition, carrier generation, carrier transport, charge trapping, and defect formation depend on the materials used in the ICs. Sensitivity to the electrostatic effects of radiation-induced trapped charge, including device-edge and inter-device leakage currents, depends on the detailed device geometries and doping profiles. Single-event effects change with scaling, including effects such as multiple-bit upsets and complicated angular effects. This paper discusses simulation-based approaches for analyzing radiation effects in advanced technologies, emphasizing multi-scale simulations that are based on detailed physical modeling of radiation interactions and carrier transport. Two major categories of radiation effects are considered: long-term and transient.

Manuscript received October 29, 2007; revised February 9, 2008. Current version published September 19, 2008.

R. D. Schrimpf, R. A. Weller, R. A. Reed, D. M. Fleetwood, and L. W. Massengill are with the Electrical Engineering and Computer Science Department, Vanderbilt University, Nashville, TN 37235 USA (e-mail: ron.schrimpf@vanderbilt.edu).

K. M. Warren, D. R. Ball, and M. A. Alles are with the Institute for Space and Defense Electronics, Vanderbilt University, Nashville, TN 37203 USA.

M. H. Mendenhall is with the Free Electron Laser Center, Vanderbilt University, Nashville, TN 37235 USA.

S. N. Rashkeev and S. T. Pantelides are with the Physics and Astronomy Department, Vanderbilt University, Nashville, TN 37235 USA.

Digital Object Identifier 10.1109/TNS.2008.2000853

A. Long-Term Effects

Exposure to radiation may produce defects that lead to long-term changes in device characteristics. The parametric shifts affect circuit and system operation, so it is necessary to analyze these effects in a unified way that includes material, device, and circuit implications. The total ionizing dose primarily affects insulating layers, in the form of deeply trapped charge or interface traps. Non-ionizing energy loss leads to displaced atoms in both insulator and semiconductor regions. In technologies with relatively large feature sizes, these effects were well described by a spatially uniform representation of the cumulative amount of energy deposited. The accuracy of this description relies on the relatively large size of the devices compared to the volume in which energy is deposited by individual particles or photons; in very small devices (less than approximately 130 nm), this approach is no longer valid [1], [2].

Oxide trapped charge (described by the areal number density projected to the Si/SiO_2 interface, N_{ot}) refers to radiation-induced charges, typically net positive, that are relatively stable. In ultrathin, high quality gate oxides, effects of oxide-trapped charge are minimal because of the small volume in which charge is generated and the ease with which it can be neutralized by tunneling. However, the current generation of high-κ dielectrics is more susceptible to ionizing radiation than thermal oxides of comparable effective thickness [3]–[5]. In state-of-the-art MOS integrated circuits (ICs), field oxides and isolation structures usually exhibit greater radiation-induced degradation than the active device regions [6].

Ionizing radiation also results in formation of interface traps (described by the areal number density, N_{it}) at semiconductor/insulator boundaries that exchange charge with the semiconductor on relatively short time scales. In MOSFETs, interface traps stretch out the subthreshold I-V characteristics and reduce the inversion-layer mobility. In BJTs, the current gain decreases with total dose due to increased surface recombination caused by Shockley-Read-Hall recombination [7]. Border traps are defects that are similar to oxide traps in microstructure, but electrically behave like slow interface traps [8].

The non-ionizing energy deposited by particle irradiation displaces atoms and creates electrically active defects. These defects reduce carrier lifetimes and mobilities, change carrier densities, and increase non-radiative transitions in optical devices, among other effects. Although majority-carrier devices, such as MOSFETs, are relatively insensitive to displacement damage, minority-carrier devices, such as BJTs, may degrade significantly.

B. Transient Effects

While the total-dose hardness of commercial ICs has generally improved in recent years [9], primarily because of reductions in gate oxide thicknesses and increases in doping densities, reduced device dimensions and accompanying technological changes have increased the sensitivity to transient radiation effects in many technologies [10]. Transient effects can be caused by individual ionizing particles (single-event effects) or high dose-rate ionizing radiation ($\dot{\gamma}$ radiation).

Single-event effects (SEEs) are a serious problem for electronics operated in space. They also are becoming an issue for advanced technologies in avionics, and even at sea level [10]. The charge deposited by a single ionizing particle can produce a wide range of effects, including single-event upset, single-event transients, single-event functional interrupt, single-event latchup, single-event dielectric rupture, and others. In general, the sensitivity of a technology to SEE increases as device dimensions decrease and as circuit speed increases [11]. These effects can be produced by direct ionization or by secondary particles resulting from nuclear reactions or elastic collisions. Recent experimental results from heavy ion and proton irradiations of advanced devices have demonstrated unpredictable SEE responses (e.g., [12]).

In a high dose-rate environment, energy is deposited relatively uniformly throughout the IC. The photocurrents that occur as the charge is collected at circuit nodes produce effects that include rail-span collapse, cell upset, and burnout of metal lines [13].

C. Multi-Scale Modeling of Radiation Effects

A comprehensive approach for simulating radiation effects requires tools that describe physical processes at the following levels:

- a quantitative description of the relevant radiation environment (particle flux, energy, angular distribution, etc.),
- transport of the incident radiation through any materials or structures that surround the sensitive circuitry (spacecraft, boxes, electronic packages, metallization, etc.),
- energy deposition in the electronic materials by the impinging radiation,
- conversion of energy into charge or defects,
- charge transport and recombination in the semiconductor and insulator regions,
- transport and reactions of other species involved in radiation effects, particularly protons and other forms of hydrogen,
- charge trapping in insulators,
- interface-trap formation,
- descriptions of the electrical effects of radiation-induced defects (trap energy levels, capture cross sections, etc.),
- device simulations, including the effects of charge deposited by the incident radiation,
- circuit simulations, including radiation-induced transients and parametric degradation, and
- system simulations, including behavioral modeling and survivability analysis.

Typically, each of these issues is considered separately in simulations; for example, models of interface-trap formation may not be directly linked to device-response simulations. However, as technologies scale and new materials are introduced, it becomes more important to have each level of simulation be informed by the levels of simulation that surround it. Multi-scale simulations can either include direct links between various types of simulations or represent the results of one level of simulation in a compact form that can be used as the input or basis for a subsequent level of simulation. Structuring the interactions between levels of simulation in a hierarchical manner provides advantages in efficiency, as well as offering design insight. In this paper, we provide brief descriptions of multi-scale simulation as applied to two radiation-effects problems: enhanced low-dose-rate sensitivity (ELDRS) in bipolar transistors and single-event effects in CMOS ICs.

II. Simulating Enhanced Low-Dose-Rate Sensitivity

A. The ELDRS Phenomenon

For bipolar transistors fabricated in some technologies, the amount of degradation at a given total dose depends on the rate at which the dose is accumulated, with more degradation occurring at lower dose rates [14]–[23]. This phenomenon is referred to as Enhanced Low-Dose-Rate Sensitivity (ELDRS). The amount of degradation typically varies most rapidly with dose rate somewhere between 0.1 and 10 rad(SiO_2)/s [18]. Dose-rate sensitivity is technology-dependent, so it is important to understand the underlying physical mechanisms in order to improve hardness and increase confidence levels.

Laboratory irradiation is frequently conducted at dose rates of 50 rad(SiO_2)/s or higher in order to complete the tests in a reasonable amount of time. However, this is significantly above the dose rates at which ELDRS typically occurs. In contrast, dose rates in space systems vary dramatically depending on orbit and shielding, but values below 0.01 rad(SiO_2)/s are typical. This can lead to overestimation of device lifetime if high dose rate tests are used to predict space-system behavior.

ELDRS is typically observed only in relatively low quality oxides irradiated at low electric fields. Oxides covering the base region of BJTs frequently satisfy these conditions because they may be thick, may not have an electrode covering the oxide, and may have been used as an implant mask. At low dose rates, the net positive oxide charge and the interface-trap density are both greater in some bipolar base oxides [24]. Thermally-stimulated current (TSC) measurements show that the apparent higher density of positive oxide charge associated with ELDRS may be due to more compensation of trapped holes by electrons, rather than reduced hole trapping [24].

B. Physical Mechanisms of ELDRS

There are three general categories of explanations that have been proposed for ELDRS: (1) space charge-related effects [23]–[29], (2) bimolecular processes [30]–[33], and (3) binary reaction rate processes [34]. Each of these models agrees with a significant amount of experimental data, at least for some devices and irradiation conditions. Given the complexity of the phenomenon, it is possible that multiple mechanisms affect the occurrence of ELDRS, perhaps even simultaneously.

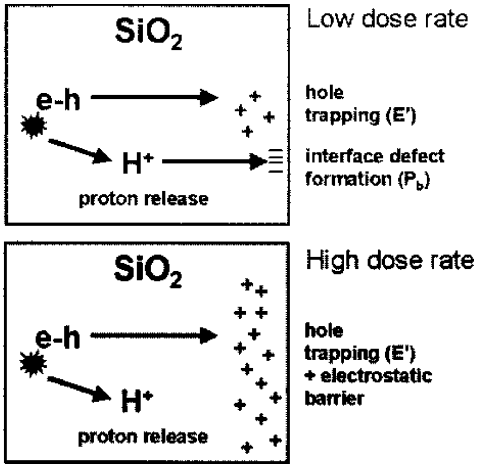

Fig. 1. Schematic comparing the buildup of interface traps at low and high dose rates [37].

In the example considered here, we focus specifically on issues associated with space-charge effects due to slowly-transporting holes [23]–[27], [35]. Hole transport is mediated by shallow traps in the oxide, while electrons in the oxide are more highly mobile and disappear at short times. The space charge that exists at higher dose rates retards the transport of holes (and also protons) to the interface. The positive charge in the bulk of the oxide causes the electric field to increase near the interface. At high dose rates (with many transporting and shallowly trapped holes in the oxide), the field changes sign near the middle of the oxide, becoming negative in the portion of the oxide far from the interface [26]. This field reversal phenomenon reduces the number of holes and protons that can reach the interface.

A critical dose rate exists at which the space charge has a significant effect on the electric field in the oxide. At dose rates far above or far below this, the charge buildup is nearly independent of dose rate. The transition between the two regions results in an s-shaped curve of excess base current vs. dose rate, as observed experimentally. Since both holes and hydrogen ions are affected by the space charge, this model applies to the dose-rate dependence observed experimentally in the buildup of both oxide charge and interface traps [27].

The transport properties of holes and protons play critical roles in determining whether a given technology will exhibit ELDRS [27]. The effective mobility of protons in the oxide is usually much lower than that of holes (several orders of magnitude difference). At low dose rates, many of the protons are able to reach the interface, release hydrogen, and form interface traps before enough holes have been trapped to reverse the field and prevent additional protons from reaching the interface. However, at high dose rates, many holes reach the interface and are trapped there before a significant number of protons are able to arrive. These holes form a sort of "electrostatic fence" that suppresses proton arrival and interface-trap formation. It is this electrostatic phenomenon, illustrated in Fig. 1, that we consider here from the perspective of multi-scale simulation.

Other mechanisms that may contribute to ELDRS also have been identified. For example, competition between trapping and recombination processes can affect the dose-rate response [24], [32], [33]. Due to trapping, some of the radiation-generated electrons remain in the oxide sufficiently long that they can recombine with transporting holes. The probability of electron trapping is much higher at low electric fields, so more of the electrons recombine under these conditions, reducing the effective charge yield. Since the carrier concentrations in the oxide are larger at high dose rates, the fraction of the carriers that recombine is greater. The increased recombination is manifested as reduced defect formation at high dose rates. It also has been suggested that ELDRS may be a delayed reaction rate effect [34], [36]. This has been described by a model that assumes that the degradation results from interaction of two species, with different times required for the species to reach the Si/SiO_2 interface [34], [36].

C. Physically-Based ELDRS Simulation

In this section, we describe how first-principles calculations can be used to obtain information that can be used in conjunction with higher-level simulations to analyze the ELDRS phenomenon. The rate equations for electrons, holes, and protons, plus Poisson's equation, build on these results to describe experimental results, including the dependence of ELDRS on the external electric field [27]. A quantitative description of the formation of radiation-induced traps at the $Si–SiO_2$ interface requires both knowledge of the physical mechanisms that underlie the phenomenon, as well as numerical simulation of the evolution of the physical system. In this case, the first-order physical mechanisms responsible for radiation-induced interface defect formation were obtained from first-principles calculations related to the release of hydrogen [38] and the reactions it undergoes when it arrives at the $Si–SiO_2$ interface [39], [40].

The method used to analyze defect formation at the atomic level is first-principles density functional theory (DFT) in the local density approximation (LDA), using large periodic supercells to achieve isolated point defects. In DFT, the total energy of the system is expressed in terms of the charge density, rather than the wavefunctions [41], [42]. The energy functional is minimized to find the ground state energy of a given atomic configuration. The structure is then relaxed and the process is iterated until the forces on the ions are less than 0.1 eV/Å. Ultra-soft pseudopotentials [43] are used for all atoms. Reaction energies are calculated by comparing energies of defect-containing supercells such that both the number of charges and number of atoms balance for the reaction. For example, the binding energy of a hydrogen atom to a nonbridging oxygen atom can be calculated as the difference in energy of two supercells, one with the hydrogen attached to the oxygen and one with the hydrogen in the main void.

Density functional theory calculations were used to identify the mechanisms responsible for interface-trap generation so that they could be incorporated in a set of differential equations describing device-level behavior. The most common process for interface-trap formation comprises the following steps [44]: (1) release of hydrogen trapped in the oxide by radiation-generated holes, (2) transport of the hydrogen (typically in the form of protons) to the Si/SiO_2 interface through drift or diffusion, (3) reaction of the protons with hydrogen-passivated defects at the

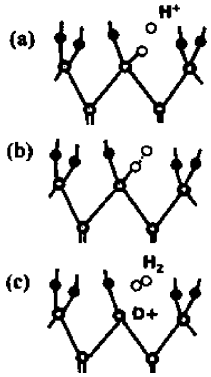

Fig. 2. Reaction between H+ and an interfacial Si-H bond [37].

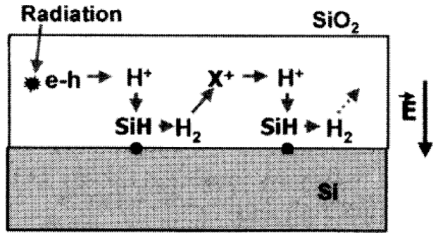

Fig. 3. Steps involved in the formation of radiation-induced interface traps [37].

interface, forming H_2 molecules and electrically active defects [37], [39], [40], and (4) transport of the H_2 molecules away from the interface. One of the key results obtained from the DFT calculations is that protons arriving at the interface do not get neutralized by electrons from the Si. Instead, the arriving protons react directly with hydrogen-passivated silicon dangling bonds [37], [40]. This process is illustrated in Fig. 2; the complete set of steps involved in forming radiation-induced interface traps is shown in Fig. 3. Fig. 2 shows a proton (H^+) (a) arriving at the interface, (b) reacting with an H-passivated dangling bond, and (c) forming a positively charged defect (D^+) and H_2, which is free to move within the semiconductor. Fig. 3 shows that this process can repeat itself if the H_2 is subsequently cracked at a site in the oxide (X^+), releasing a proton that can depassivate another interface trap.

The proton transport process and interfacial reactions related to interface-trap formation were incorporated in a multiple-trapping-detrapping (MTD) code similar to the one used in [26] to study the dose-rate dependence of oxide trapped charge buildup. Hole and proton transport were described using drift-diffusion equations; more complicated dispersive transport simulations yielded similar results. In this way, we can compare the transport of holes and protons conveniently using the concept of effective mobility.

An example of the results is shown in Fig. 4, which illustrates oxide-trapped charge density vs. dose rate for irradiated MOS capacitors. This figure compares the results of the physically-based numerical model described here and an analytical model based on the same mechanisms. The hole and proton mobilities used in the simulations were $\mu_p = 10^{-5}$ cm^2/Vs and $\mu_{H+} = 10^{-11}$ cm^2/Vs. In these results the applied electric field in the

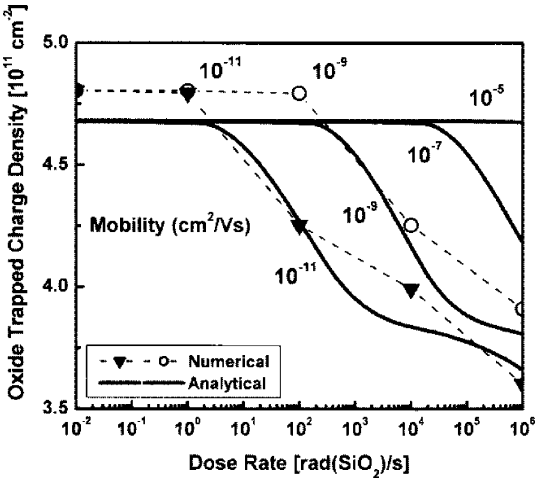

Fig. 4. Oxide trapped charge density vs. dose rate for irradiated MOS capacitors [27].

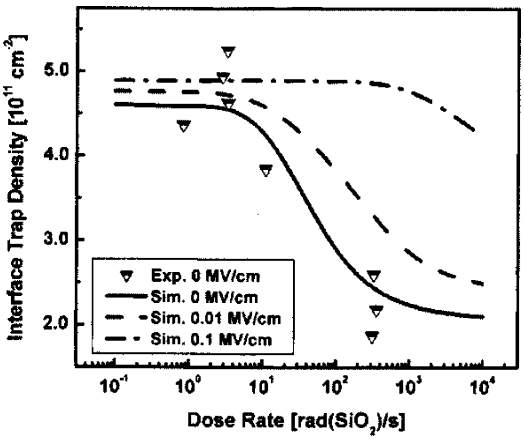

Fig. 5. Interface-trap density vs. dose rate for three values of electric field (obtained from simulation) compared to zero-bias experimental data [37].

oxide is zero. At low dose rates, more of the holes are able to reach the interface, as seen by the higher value of oxide-trapped charge. However, at high dose rates, the space charge due to the transporting holes suppresses oxide-trapped charge.

The electric field has a significant effect on ELDRS, with high values of field tending to suppress the occurrence of ELDRS. Fig. 5 shows the results of simulations for a typical range of electric field values compared to experimental data for an Analog Devices RF25 capacitor irradiated to a total dose of 200 krad(SiO_2). For example, a typical bias of $V_{BE} = 0.6$ V corresponds to an electric field in the base oxide of approximately 0.1 MV/cm in these devices. At high values of electric field, the ELDRS effect is less pronounced because it is harder to reach the field reversal regime; thus, all the generated positive charges reach the interfacial region where they get a chance to react and create interface traps. In this case, the concentration of radiation-induced traps is independent of the dose rate.

It has also been demonstrated that pre-irradiation elevated temperature stress (PETS) and aging can affect the apparent dose-rate and time-dependent response of linear bipolar devices [45], [46]. For example, in some cases PETS can reduce, or

even eliminate, ELDRS. In addition, the radiation and subsequent annealing responses of interface traps in MOS transistors can change significantly during long-term aging [46]. Thus, it can be difficult to distinguish true or apparent dose rate effects from changes in device radiation response due to aging effects during a low-dose-rate radiation exposure. ELDRS also is known to depend strongly on the nature of the passivation layers in the device, particularly on the hydrogen content of the passivation layers and their ability to prevent additional hydrogen from reaching the Si/SiO_2 interface [47]. All of these effects seem to be primarily due to changes in concentration, transport, and reactions of hydrogenous species, which can be affected strongly by device processing, packaging, and time-temperature history. Simulations have been performed that illustrate that water contained in the SiO_2 layers is one possible source of hydrogen that can affect radiation-induced interface-trap formation [48]. Future work is necessary to extend these efforts to include the effects of H_2 and other hydrogenous species to obtain a more complete understanding of ELDRS related effects in linear bipolar ICs.

D. Conclusions: Multiscale Simulation of Parametric Degradation

Design and fabrication of electronic systems for space has traditionally been performed using an iterative process in which designers postulate a solution, fabricate it, test it, and compare the results to the design specifications. However, this approach is expensive, time-consuming, and frequently inaccurate. A potential solution to this problem is to develop models that capture the relevant physics, simultaneously allowing alternative designs to be evaluated and providing insight into improved designs. However, at present it is difficult to perform truly integrated multi-scale simulations of total-dose effects. As illustrated in the example described here, it is possible to use a hierarchical multi-scale modeling approach in which the relevant physical phenomena are captured at each level of the modeling hierarchy and used to inform simulations at the higher levels. While this type of loosely-coupled simulation does not provide an end-to-end prediction of the radiation response of complex devices operating in realistic environments, it does emphasize the physical insight that can be obtained through identifying and quantifying key parameters at each level of simulation. As demonstrated in the following section, it currently is possible to use a more fully integrated approach for simulating single-event effects in electronics.

III. Simulating Single-Event Effects

A. Introduction

As microelectronic technologies become smaller, faster, and denser, it becomes important to understand the detailed mechanisms responsible for single-event effects. The circuit response depends on the amount of charge collected by sensitive nodes and the rate at which the charge is collected. The presence of high-Z metallization layers, like tungsten or copper, or materials with very large neutron cross sections, like Boron-10, may strongly impact the single-event error rate [49]–[54]. Also, circuits designed to be immune to charge collection at a single circuit node [55] may still be vulnerable to upset caused by charge collection at multiple nodes.

Single-event effects analysis and simulation are typically based on average particle strikes, described by the stopping power, or linear energy transfer (LET), of the incident particle. The linear energy transfer in electronic materials is a measure of the energy that is converted to electron-hole pairs per path length and the units are typically $\mathrm{MeV\text{-}cm^2/mg}$. These units result from dividing the amount of ionizing energy deposited per path length by the density of the material in which the energy is deposited. In Si, one electron-hole pair is created for each 3.6 eV of ionizing energy deposited [56]; the corresponding value for SiO_2 is $\sim 17\ \mathrm{eV}$ [57].

Although LET is a useful concept in many common situations, the amount of energy deposited in a sensitive device volume due to a particular event, as well as the spatial and temporal distribution of the deposited energy, may vary significantly even when considering a group of particles having the same mass and incident energy. Thus, the average deposited energy per particle does not necessarily determine the response of the circuit to that type of particle. If the mean LET lies below a threshold necessary to produce effects due to direct ionization, the measured circuit response will be determined by the fraction of particles that deposit enough energy in the sensitive region of the circuit to produce measurable effects. In particular, the results of calculations based only on LET will be very misleading when a significant portion of the relevant effects are initiated by nuclear reactions.

In the example presented here, we describe a method for simulating large numbers of realistic single events using custom software tools based on the Geant4 Monte Carlo model library to describe the energy-deposition processes and Technology Computer Aided Design (TCAD) tools for device and circuit simulations. The results of these simulations show that event-to-event variation may have a significant impact when predicting the single-event error rate in advanced spacecraft electronics.

B. Simulation Approach

The approach for simulating single-event effects described here is based on detailed descriptions of large numbers of individual particle interactions [1], [58]. Spatially and temporally realistic representations of the charge deposited by individual energetic particles are used as input for device simulations [59], which in turn are used to determine the circuit-level response. By considering a large number of events initiated by individual primary radiation quanta and studying device response to these individual events, this approach allows us to obtain both average device response and statistical variability. Unlike the radiation-effects simulation methods commonly used, mechanisms that depend on the microstructure of radiation interactions with highly scaled and emerging devices, such as multiple bit upsets, secondary radiation from materials near active devices [49], [60], microdose effects [61], and highly localized displacement damage, can be analyzed quantitatively. An overview of this approach is illustrated in Fig. 6 [58]. The

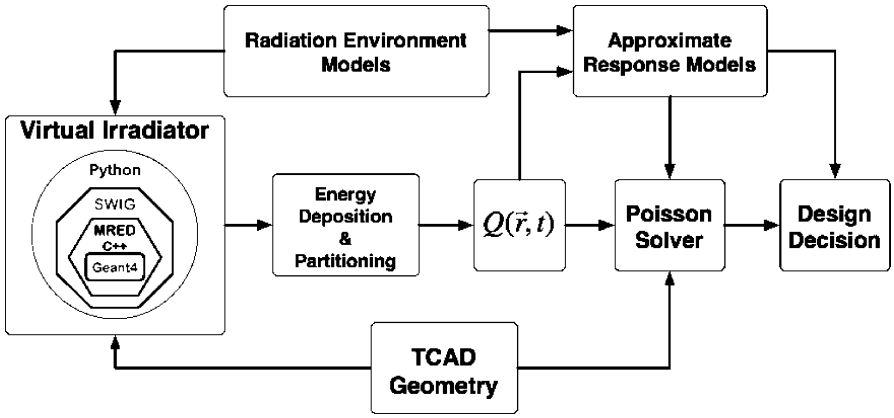

Fig. 6. Block diagram of the RADSAFE simulation environment [58].

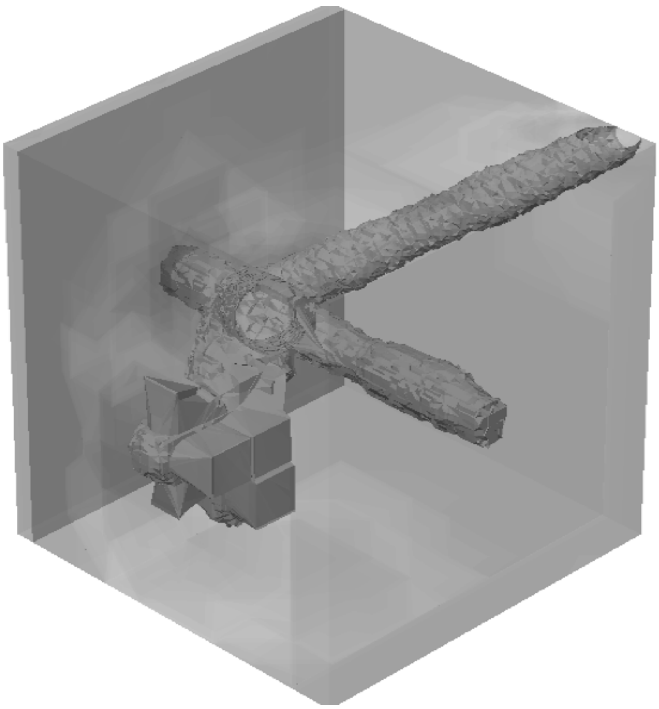

Fig. 7. Charge deposited in a Si cube by an ion-induced nuclear reaction. The electron concentration at the iso-charge surfaces is 10^{14} cm^{-3} [58].

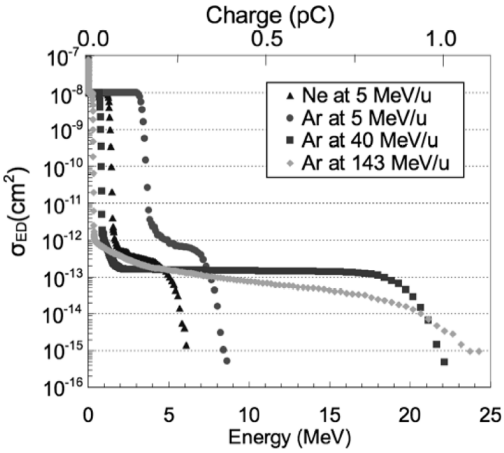

Fig. 8. Energy-deposition cross section vs. energy for Ne and Ar ions incident on a block of Si containing a 1 μm^3 sensitive volume [64].

overall multiscale-simulation environment, as implemented at Vanderbilt University, is called RADSAFE.

In this implementation, the virtual irradiator uses MRED (Monte Carlo Radiative Energy Deposition), a custom application based on Geant4 [62]. MRED is a custom application based on the Geant4 libraries [62], which include computational physics models for the transport of radiation through matter. Geant4 is a library of c++ routines assembled by an international collaboration for describing radiation interaction with matter. MRED includes a model for screened Coulomb scattering of ions [63], tetrahedral geometric objects [60], a cross section biasing and track weighting technique for variance reduction, and a number of additional features relevant to semiconductor device applications. The Geant4 libraries frequently contain alternative models for the same physical processes, which may differ in levels of detail and accuracy. Some of the models contained in Geant4 currently are not valid at the nanoscale, but the organization of Geant4 allows these models to be replaced or improved as improved models are developed. Generally, MRED is structured so that all physics relevant for radiation effects applications are available and selectable at run time.

The virtual irradiator requires descriptions of the radiation environment, as well as the geometry and composition of the device to be analyzed. MRED is used to generate very large numbers of individual event descriptions. These events are intrinsically three-dimensional and the resulting particles may include electrons, protons, neutrons, other subatomic particles, larger atomic fragments, and photons. MRED provides the amount of energy for each particle as a function of space and time, along with the fraction of the energy that results in ionization. Custom tools are used to process this information and convert it to a 3-D charge distribution that is automatically meshed for use in a device simulation tool; an example is shown in Fig. 7, which was generated by simulating 1 GeV/nucleon ^{12}C ions incident on a $5 \times 5 \times 5$ μm^3 Si cube. The surfaces in this figure are iso-concentration surfaces at which the electron concentration is 10^{14} cm^{-3}. Charge tracks corresponding to several reaction products are seen, illustrating the complexity of the charge

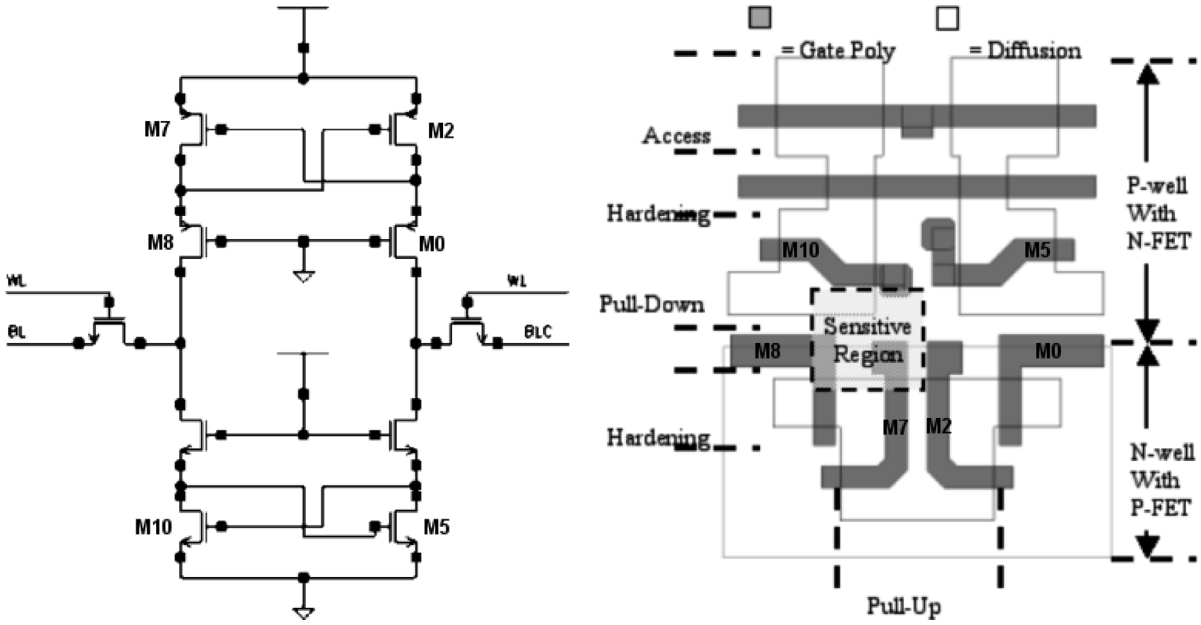

Fig. 9. Layout and schematic of the 10-T SRAM analyzed in the example described here [65].

distribution that may result from this type of event. The device-simulation tool accepts the radiation-generated charge as input and provides terminal currents vs. time, and if the device is embedded in a circuit, the occurrence of an upset can be determined. Analysis of a large number of these events allows determination of higher-level representations of circuit response, such as upset cross-section vs. incident particle characteristics. It also is possible to create a database of event descriptions that can be used in subsequent simulations without having to run the Geant4-based code each time.

C. Event-Rate Calculations

Fig. 8 presents an example of how MRED can be used to estimate the event rate of a circuit if the critical charge required to produce an event is known [64]. The sample used for this calculation is a silicon cube that is 30 μm on a side, with a sensitive volume consisting of a 1 μm^3 cube, centered 10.5 μm below the top surface. There is a 0.5 μm layer of tungsten just above the sensitive volume, representing the presence of a via above the sensitive volume. The data points represent the computed cross section, $\sigma_{ED}(E)$, for depositing an energy E or greater in the sensitive volume for ions normally incident on the top surface of the sample. Results are included for 5 MeV/u Ne ions and 5, 40, and 143 MeV/u Ar ions. Each ion has an LET between 1.5 and 13.7 MeV-cm^2/mg. The SEE cross section, σ_{SEE}, can be determined from $\sigma_{ED}(E)$ by evaluating it at the critical charge required to produce an upset, Q_{crit}, where the critical energy is related to the critical charge by $E_{crit} = Q_{crit} \times 22.5$ MeV/pC.

$$\sigma_{SEE} = \sigma_{ED}\left(E_{crit}\right). \tag{1}$$

The abrupt decrease in each cross-section curve at low energy corresponds to the transition from energy deposition by direct ionization at low energy to that by indirect ionization at higher energy. These results show that the measured σ_{SEE} of a circuit that has a high critical charge would depend strongly on the ion energy. For example, a circuit with a critical charge for SEU of 0.5 pC would exhibit a significant number of upsets if exposed to 40 MeV/u argon ions. However, no SEUs will occur if the circuit is exposed to 5 MeV/u argon ions, even though the 5 MeV/u ions have a greater LET than the 40 MeV/u ions (14 vs. 3.8 MeV-cm^2/mg). This decrease in LET with incident particle energy occurs because the interaction between the ion and the target decreases at high energies and it demonstrates that LET is not the relevant metric for predicting the single-event rate in this case. By irradiating devices with ions at several different energies (selected based on the results of the simulations), an experimenter can use accelerator testing to identify if nuclear reactions will contribute to the measured SEE cross section.

D. Event-Rate Estimation for an SRAM

In this example, the event rate for an SRAM cell is estimated, including the effects of overlayers (metal and interlevel dielectrics), using MRED to produce realistic nuclear events [65]. These events were used as input into TCAD electrical simulations to determine the device and circuit response to the event and then compared to a standard heavy-ion model based on direct ionization. Charge deposition due to the nuclear events greatly exceeds the charge deposition expected based on the LET of the primary ion.

The technology considered in this work is a radiation-hardened 4-Mbit SRAM, each cell consisting of 10 transistors, with a supply voltage of 3.3 V. This is a dual well bulk CMOS process and the minimum drawn gate length is 0.4 μm. There are three layers of metal available in the process. The schematic and layout of the 10-T cell are shown in Fig. 9.

The SEU cross section was measured vs. LET at the Texas A&M cyclotron using species ranging from 523 MeV Ne (LET of 1.79 MeV-cm^2/mg) to 2000 MeV Au (LET of 87.1 MeV-cm^2/mg), as shown in Fig. 10. All the ions used to

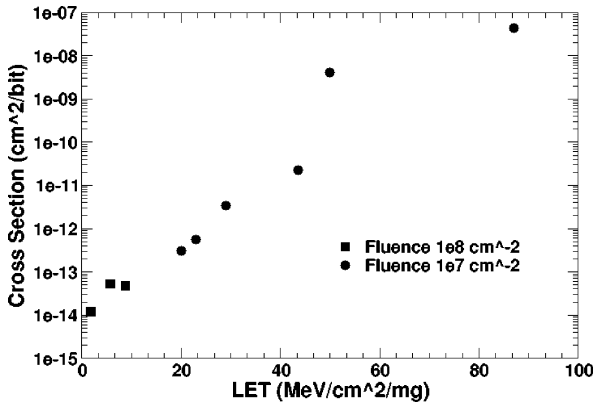

Fig. 10. SEU cross section vs. LET for a 4M SRAM circuit [65].

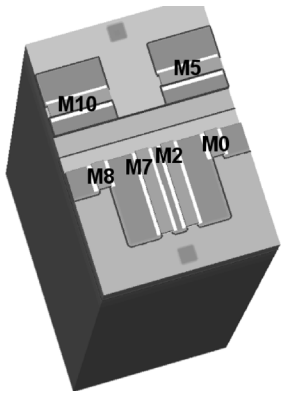

Fig. 11. 3-D simulation structure used to analyze single-event effects in the 10-T SRAM cell [65].

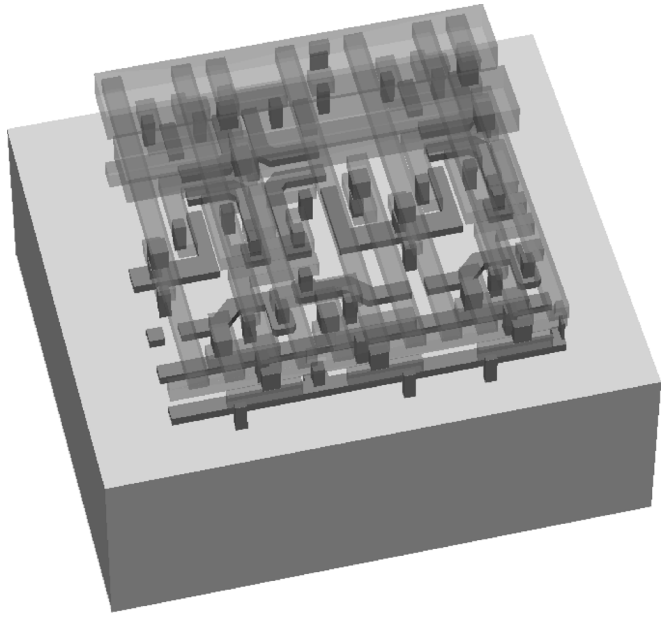

Fig. 12. 3D model of the SRAM cell, illustrating the polysilicon, metal layers and tungsten plugs [65].

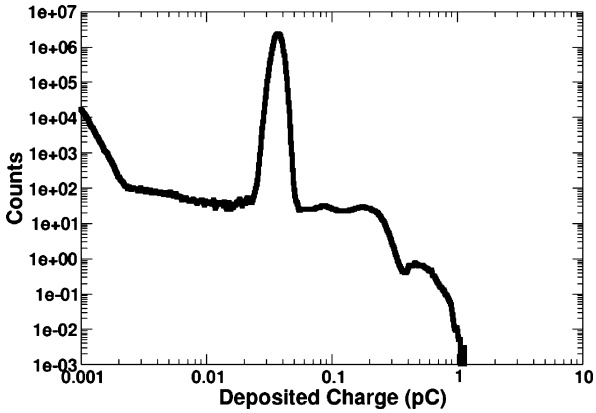

Fig. 13. Histogram representing the number of events depositing a given amount of charge in the sensitive volume of the SRAM [65].

construct Fig. 10 were normally incident, so the x-axis is actual particle LET rather than effective LET. The upset threshold for this circuit is not clearly defined; the cross section decreases gradually as the LET decreases. Two-photon absorption [66], [67] was used to identify the regions in the circuit that are sensitive to single event upset and a single region was identified as responsible for the upsets that occur near the upset threshold. This sensitive area is shown on the right side of Fig. 9.

A 3D model of a portion of the SRAM is shown in Fig. 11. The physical model includes all four PMOS transistors and the two pull-down NMOS transistors. The remaining circuit elements in the SRAM were modeled using SPICE BSIM3V3 models. First, the SRAM was analyzed using a traditional LET-based model in which a specified amount of charge per unit path length is deposited. This method represents only charge generated by direct ionization. The lowest LET at which simulated upsets were observed was 50 MeV-cm^2/mg. However, the data presented in Fig. 10 show that the SRAM is sensitive to ions with an LET of less than 50 MeV-cm^2/mg. These results show that considering only direct ionization does not describe all of the upset mechanisms that may occur in this memory cell.

The mechanisms responsible for the low-LET upsets were examined using MRED. Using vendor-supplied layout files, a simulation structure was built that included the active portion of the memory cell plus all overlayer materials. In Fig. 12, the polysilicon gates, tungsten plugs and three layers of aluminum metallization are shown. The insulating layers were present in the structure used for MRED simulations, but are not shown in the illustration for clarity. It should also be noted that this structure is used for MRED simulations; however, the presence of the overlayers is not required for the TCAD device simulations.

Charge deposition simulations were performed in MRED with the complete structure as the target. A mono-energetic beam of 523 MeV ^{20}Neon ions was randomized over the structure at normal incidence. This ion was chosen as the test case because it represented the lowest LET (1.79 MeV-cm^2/mg) that experimentally produced upsets in the SRAM. The results of 1×10^8 simulation events are shown in Fig. 13. The total energy deposited in the entire structure for each of the particles was binned and used to generate the charge deposition spectrum. For the given sensitive volume depth, the data in Fig. 13 yield an average LET of 1.79 MeV-cm^2/mg. However, the data also show that there are some events that deposit more than 1 pC of charge.

The events occurring in the peak around 35 fC are due to direct ionization by the primary ion; the high-energy deposition events are due to a combination of direct ionization and indirect ionization events. The events depositing the most charge are equivalent to an apparent LET of approximately 50 MeV-cm^2/mg (apparent LET is significant only for comparison to the true LET of the primary ion and does not directly refer to the stopping power of any secondary species). These results demonstrate that a primary ion with an LET of 1.79 MeV-cm^2/mg can produce an indirect ionization event that deposits as much charge as a primary ion with an apparent LET of 50 MeV-cm^2/mg.

Simulating the response of a device to a realistic charge track that involves multiple ionizing particles is more complicated than simulating the response to a charge track with uniform LET. At Vanderbilt, code has been developed that takes the physical description of the nuclear event from MRED, and creates a mesh suitable for device simulation. The code also generates the correct number of electron-hole pairs corresponding to the energy deposition.

The TCAD simulations showed that slightly more than 1 pC of charge deposited in the sensitive volume can cause the SRAM to upset. Using 523 MeV ^{20}Neon ions with an LET of 1.79 MeV-cm^2/mg as the primary species, the SRAM was bombarded with a billion events and an event was chosen for detailed device simulations that deposited over 1 pC of charge into the sensitive region. This event was used as the input to a mixed-mode device simulation, and was enough to cause the SRAM to upset [65].

Because of the complexity of simulating realistic charge tracks in TCAD tools, simplified methods of representing device SEE response are desirable. One such approach is based on defining multiple sensitive volumes, each with its own charge-collection efficiency [68]. The charge collected at a given circuit node is obtained by summing the charge deposited in each of the sensitive volumes associated with that node, scaled by the charge-collection efficiency of each sensitive volume. Using this approach, with limited calibration to heavy-ion data, the response of an SRAM in a realistic environment was estimated [69]. This estimate included the effects of particle type, energy, and angle of incidence.

E. Multiple-Bit Upsets

The multi-scale simulation approach described here also can be used to determine the number of events that deposit at least a specified amount of energy in more than one sensitive volume [70]. This is important for determining the number of multiple-bit upsets that occur in a memory or for determining the upset vulnerability of a cell that is immune to charge deposition at a single node, but can be upset by simultaneous charge deposition at two or more nodes [55]. Fig. 14 is an example of a multiple-bit upset in a 130-nm CMOS memory produced by a 63-MeV proton that causes a nuclear reaction. Each shaded box represents the sensitive volume of one memory cell. In this particular case, the incident proton enters at a grazing angle and reacts with the silicon to cause a nuclear event. Among the reaction products is a 14-MeV oxygen ion that traverses six, darker shaded, sensitive volumes. The amount of charge deposited in each sensitive volume is indicated in the figure.

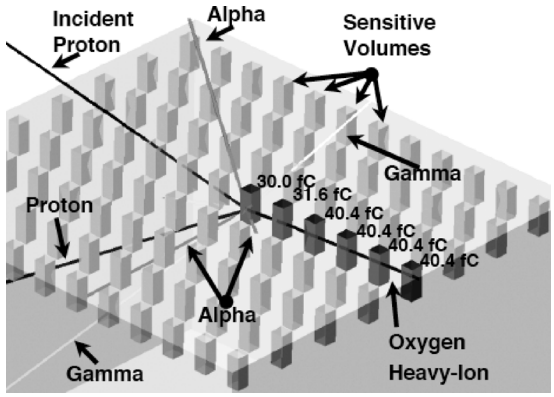

Fig. 14. Energy deposition in a 130-nm CMOS memory caused by a proton-induced nuclear reaction [70]. The oxygen ion produced by the reaction upsets six bits.

For typical values of critical charge, all six of the cells traversed by the oxygen ion will be upset.

F. Conclusions: Multi-Scale Simulation of Single-Event Effects

For older technologies (minimum feature sizes ≥ 0.5 μm), it was usually sufficient to predict SEE rates through a combination of accelerator-based experiments and simulations that use a track structure corresponding to an average event. However, this approach may yield inaccurate results in more advanced technologies, particularly those in which particle-track sizes are comparable to transistor and cell dimensions or those with complicated charge-collection mechanisms. More accurate SEE rates, as well as better insight, can be obtained by simulation of a large number of physically realistic events. The insight provided by the simulations can be used to guide experiments and identify situations in which nuclear reactions are likely to play a significant role. For the SRAM example presented above, the importance of SEU from secondary processes results from the combination of a large total sensitive volume and a relatively high critical charge. The devices most affected by this phenomenon are likely to be future generations of high density radiation-hardened memories [49]. These secondary scattering processes should be considered when evaluating the underlying cause of small cross-section, low-LET, single event upsets.

IV. Computing Requirements

The computational needs for multi-scale simulation can be very demanding. For example, the MRED simulations described above were performed on a 1500-processor supercomputer at Vanderbilt University's Advanced Computing Center for Research and Education (ACCRE). The Monte Carlo simulations that form the basis for MRED are intrinsically parallelizable—since each event can run on a single processor, the simulation throughput is directly proportional to the number of processors used. This ideal scalability allows very large numbers of events to be performed so that good statistics can be obtained. However, it is practical to run simpler MRED simulations with fewer events on an individual laptop. For MRED simulations, people typically use 100–300 cpu's. Each is an independent thread based on its

own random number sequence, and may have up to 10 or even 100 million events. Such runs take from a few minutes to a few hours depending on the complexity of the target. Generally, a MRED session can run in 1 GB of memory, unless the target is extremely complex.

We use various variance-reduction strategies to improve statistical confidence for rare events. Among the most important of these is biasing the nuclear-reaction cross sections [71]. We artificially boost these cross sections by factors of up to 1000 and simultaneously make a corresponding decrease in the statistical weight of the resulting events. If the cross section bias factor is, e.g., 200, which is a typical value, and we run 10^9 real events, which is a realistic number using 100 processors running 10^7 events each, the result is the same as if we ran 2×10^{11} events without biasing [71]. Since these all strike a small volume, we can actually run many more events than some experiments do. Other statistical techniques are used to deal, e.g, with cosmic ray environments, where the ranges of energies and fluxes cover many orders of magnitude, and where very rare events can in principle create effects out of all proportion to their numbers, as discussed above.

Likewise, availability of high performance computing (HPC) allows a more thorough examination of the design space to be performed for device and circuit simulations. In general, the time required to perform a single device simulation does not decrease dramatically when it runs on a parallel supercomputer. However, many simulations can be performed in parallel and all of the results can be obtained at the same time, rather than sequentially. This makes it practical to set up a matrix of designs to assess the vulnerability of various device or circuit options. If more modest computing resources are available, it becomes important to look for overall trends in the simulation results and choose specific designs based on experience.

V. Summary

Simulations have become an indispensable element in radiation-effects analysis. Simulation tools allow consideration of complex geometries that cannot be considered analytically and examination of quantities that cannot be measured directly. The full benefit of simulation can only be realized if the models used at every level are physically based. However, it is not practical, or even desirable, to simulate complicated integrated circuits at the level of individual atoms. By using multi-scale simulations, the most significant effects can be captured at each level and passed in compact form to simulation tools operating at higher levels of abstraction. Two examples were considered in this overview: enhanced low-dose-rate sensitivity in bipolar transistors and single-event effects in CMOS circuits. In the case of ELDRS, the important atomic-scale processes were identified using density functional theory and device-level simulations based on these processes were used to interpret the experimental data. For SEE, a Monte Carlo-based simulation tool was used to generate detailed descriptions of individual events that were used as the input for device and circuit simulations. These multi-scale simulations provide insight that is difficult to obtain from more empirical approaches.

References

[1] R. A. Weller, A. L. Sternberg, L. W. Massengill, R. D. Schrimpf, and D. M. Fleetwood, "Evaluating average and atypical response in radiation effects simulations," *IEEE Trans. Nucl. Sci.*, vol. 50, no. 6, pp. 2265–2271, Dec. 2003.

[2] R. A. Weller, R. D. Schrimpf, R. A. Reed, A. L. Sternberg, A. S. Kobayashi, M. H. Mendenhall, L. W. Massengill, and D. M. Fleetwood, "Modeling semiconductor device response using detailed radiation event simulations," in *Proc. Hardened Electron. Radiation Technol. Conf.*, Monterey, CA, 2004.

[3] J. A. Felix, D. M. Fleetwood, R. D. Schrimpf, J. G. Hong, G. Lucovsky, J. R. Schwank, and M. R. Shaneyfelt, "Total-dose radiation response of hafnium-silicate capacitors," *IEEE Trans. Nucl. Sci.*, vol. 49, no. 6, pp. 3191–3196, Dec. 2002.

[4] J. A. Felix, H. D. Xiong, D. M. Fleetwood, E. P. Gusev, R. D. Schrimpf, A. L. Sternberg, and C. D'Emic, "Interface trapping properties of Al_2O_3/SiO_xN_y/Si(100) NMOSFETs after exposure to ionizing radiation," *Microelectron. Eng.*, vol. 72, pp. 50–54, 2004.

[5] J. A. Felix, M. R. Shaneyfelt, D. M. Fleetwood, T. L. Meisenheimer, J. R. Schwank, R. D. Schrimpf, P. E. Dodd, E. P. Gusev, and C. D'Emic, "Radiation-induced charge trapping in thin Al_2O_3/SiO_xN_y/Si[100] gate dielectric stacks," *IEEE Trans. Nucl. Sci.*, vol. 50, no. 6, pp. 1910–1918, Dec. 2003.

[6] M. Turowski, A. Raman, and R. D. Schrimpf, "Nonuniform total-dose-induced charge distribution in shallow-trench isolation oxides," *IEEE Trans. Nucl. Sci.*, vol. 51, no. 6, pp. 3166–3171, Dec. 2004.

[7] R. D. Schrimpf, "Gain degradation and enhanced low-dose-rate sensitivity in bipolar junction transistors," *Int. J. High Speed Electron. Syst.*, vol. 14, pp. 503–517, 2004.

[8] D. M. Fleetwood, "'Border traps' in MOS devices," *IEEE Trans. Nucl. Sci.*, vol. 39, no. 2, pp. 269–271, Apr. 1992.

[9] R. C. Lacoe, J. V. Osborn, D. C. Mayer, and S. Brown, "Total-dose radiation tolerance of a commercial 0.35 μm CMOS process," in *Proc. IEEE Radiation Effects Data Workshop*, 1998, vol. NSREC 98, pp. 104–110.

[10] P. E. Dodd and L. W. Massengill, "Basic mechanisms and modeling of single-event upset in digital microelectronics," *IEEE Trans. Nucl. Sci.*, vol. 50, no. 3, pp. 583–602, Jun. 2003.

[11] P. E. Dodd, M. R. Shaneyfelt, J. A. Felix, and J. R. Schwank, "Production and propagation of single-event transients in high-speed digital logic ICs," *IEEE Trans. Nucl. Sci.*, vol. 51, no. 6, pp. 3278–3284, Dec. 2004.

[12] R. A. Reed, P. W. Marshall, H. S. Kim, P. J. McNulty, B. Fodness, T. M. Jordan, R. Reedy, C. Tabbert, M. S. T. Liu, W. Heikkila, S. Buchner, R. Ladbury, and K. A. LaBel, "Evidence for angular effects in proton-induced single-event upsets," *IEEE Trans. Nucl. Sci.*, vol. 49, no. 6, pp. 3038–3044, Dec. 2002.

[13] L. W. Massengill, S. E. Diehl, and J. S. Browning, "Dose-rate upset patterns in a 16 k CMOS SRAM," *IEEE Trans. Nucl. Sci.*, vol. NS-33, no. 6, pp. 1541–1545, Dec. 1986.

[14] E. W. Enlow, R. L. Pease, W. E. Combs, R. D. Schrimpf, and R. N. Nowlin, "Response of advanced bipolar processes to ionizing radiation," *IEEE Trans. Nucl. Sci.*, vol. 38, no. 6, pp. 1342–1351, Dec. 1991.

[15] S. L. Kosier, W. E. Combs, A. Wei, R. D. Schrimpf, D. M. Fleetwood, M. DeLaus, and R. L. Pease, "Bounding the total-dose response of modern bipolar transistors," *IEEE Trans. Nucl. Sci.*, vol. 41, no. 6, pp. 1864–1870, Dec. 1994.

[16] R. N. Nowlin, E. W. Enlow, R. D. Schrimpf, and W. E. Combs, "Trends in the total-dose response of modern bipolar transistors," *IEEE Trans. Nucl. Sci.*, vol. 39, no. 6, pp. 2026–2035, Dec. 1992.

[17] R. N. Nowlin, D. M. Fleetwood, R. D. Schrimpf, R. L. Pease, and W. E. Combs, "Hardness-assurance and testing issues for Bipolar/BiCMOS devices," *IEEE Trans. Nucl. Sci.*, vol. 40, no. 6, pp. 1686–1693, Dec. 1993.

[18] R. N. Nowlin, D. M. Fleetwood, and R. D. Schrimpf, "Saturation of the dose-rate response of BJTs below 10 rad(SiO_2)/s: implications for hardness assurance," *IEEE Trans. Nucl. Sci.*, vol. 41, no. 6, pp. 2637–2641, Dec. 1994.

[19] R. D. Schrimpf, R. J. Graves, D. M. Schmidt, D. M. Fleetwood, R. L. Pease, W. E. Combs, and M. DeLaus, "Hardness assurance issues for lateral PNP bipolar junction transistors," *IEEE Trans. Nucl. Sci.*, vol. 42, no. 6, pp. 1641–1649, Dec. 1995.

[20] A. Wei, S. L. Kosier, R. D. Schrimpf, D. M. Fleetwood, and W. E. Combs, "Dose-rate effects on radiation-induced bipolar junction transistor gain degradation," *Appl. Phys. Lett.*, vol. 65, pp. 1918–1920, 1994.

[21] S. C. Witczak, R. D. Schrimpf, K. F. Galloway, D. M. Fleetwood, R. L. Pease, J. M. Puhl, D. M. Schmidt, W. E. Combs, and J. S. Suehle, "Accelerated tests for simulating low dose rate gain degradation of lateral and substrate PNP bipolar junction transistors," *IEEE Trans. Nucl. Sci.*, vol. 43, no. 6, pp. 3151–3160, Dec. 1996.

[22] S. C. Witczak, R. D. Schrimpf, D. M. Fleetwood, K. F. Galloway, R. C. Lacoe, D. C. Mayer, J. M. Puhl, R. L. Pease, and J. S. Suehle, "Hardness assurance testing of bipolar junction transistors at elevated irradiation temperatures," *IEEE Trans. Nucl. Sci.*, vol. 44, no. 6, pp. 1989–2000, Dec. 1997.

[23] S. C. Witczak, R. C. Lacoe, D. C. Mayer, D. M. Fleetwood, R. D. Schrimpf, and K. F. Galloway, "Space charge limited degradation of bipolar oxides at low electric fields," *IEEE Trans. Nucl. Sci.*, vol. 45, no. 6, pp. 2339–2351, Dec. 1998.

[24] D. M. Fleetwood, L. C. Riewe, J. R. Schwank, S. C. Witczak, and R. D. Schrimpf, "Radiation effects at low electric fields in thermal, SIMOX, and bipolar-base oxides," *IEEE Trans. Nucl. Sci.*, vol. 43, no. 6, pp. 2537–2546, Dec. 1996.

[25] D. M. Fleetwood, S. L. Kosier, R. N. Nowlin, R. D. Schrimpf, R. A. Reber Jr., M. DeLaus, P. S. Winokur, A. Wei, W. E. Combs, and R. L. Pease, "Physical mechanisms contributing to enhanced bipolar gain degradation at low dose rates," *IEEE Trans. Nucl. Sci.*, vol. 41, no. 6, pp. 1871–1883, Dec. 1994.

[26] R. J. Graves, C. R. Cirba, R. D. Schrimpf, R. J. Milanowski, A. Michez, D. M. Fleetwood, S. C. Witczak, and F. Saigne, "Modeling low-dose-rate effects in irradiated bipolar-base oxides," *IEEE Trans. Nucl. Sci.*, vol. 45, no. 6, pp. 2352–2360, Dec. 1998.

[27] S. N. Rashkeev, C. R. Cirba, D. M. Fleetwood, R. D. Schrimpf, S. C. Witczak, A. Michez, and S. T. Pantelides, "Physical model for enhanced interface-trap formation at low dose rates," *IEEE Trans. Nucl. Sci.*, vol. 49, no. 6, pp. 2650–2655, Dec. 2002.

[28] S. N. Rashkeev, D. M. Fleetwood, R. D. Schrimpf, and S. T. Pantelides, "Effects of hydrogen motion on interface trap formation and annealing," *IEEE Trans. Nucl. Sci.*, vol. 51, no. 6, pp. 3158–3165, Dec. 2004.

[29] R. L. Pease, D. G. Platteter, G. W. Dunham, J. E. Seiler, H. J. Barnaby, R. D. Schrimpf, M. R. Shaneyfelt, M. C. Maher, and R. N. Nowlin, "Characterization of enhanced low dose rate sensitivity (ELDRS) effects using gated lateral PNP transistor structures," *IEEE Trans. Nucl. Sci.*, vol. 51, no. 6, pp. 3773–3780, Dec. 2004.

[30] V. V. Belyakov, V. S. Pershenkov, A. V. Shalnov, and I. N. Shvetzov-Shilovsky, "Use of MOS structure for investigation of low-dose-rate effect in bipolar transistors," *IEEE Trans. Nucl. Sci.*, vol. 42, no. 6, pp. 1660–1666, Dec. 1995.

[31] H. P. Hjalmarson, R. L. Pease, S. C. Witczak, M. R. Shaneyfelt, J. R. Schwank, A. H. Edwards, C. E. Hembree, and T. R. Mattsson, "Mechanisms for radiation dose-rate sensitivity of bipolar transistors," *IEEE Trans. Nucl. Sci.*, vol. 50, no. 6, pp. 1901–1909, Dec. 2003.

[32] J. Boch, F. Saigné, R. D. Schrimpf, J. R. Vaille, L. Dusseau, and E. Lorfevre, "Physical model for the low-dose-rate effect in bipolar devices," *IEEE Trans. Nucl. Sci.*, vol. 53, no. 6, pp. 3655–3660, Dec. 2006.

[33] J. Boch, F. Saigné, A. D. Touboul, S. Ducret, J. F. Carlotti, M. Bernard, R. D. Schrimpf, F. Wrobel, and G. Sarrabayrouse, "Dose rate effects in bipolar oxides: Competition between trap filling and recombination," *Appl. Phys. Lett.*, vol. 88, p. 232113, 2006.

[34] R. K. Freitag and D. B. Brown, "Study of low-dose-rate radiation effects on commercial linear bipolar ICs," *IEEE Trans. Nucl. Sci.*, vol. 45, no. 6, pp. 2649–2658, Dec. 1998.

[35] D. M. Fleetwood, M. J. Johnson, T. L. Meisenheimer, P. S. Winokur, W. L. Warren, and S. C. Witczak, "1/f noise, hydrogen transport, and latent interface-trap buildup in irradiated MOS devices," *IEEE Trans. Nucl. Sci.*, vol. 44, no. 6, pp. 1810–1817, Dec. 1997.

[36] R. K. Freitag and D. B. Brown, "Low dose rate effects on linear bipolar IC's: experiments on the time dependence," *IEEE Trans. Nucl. Sci.*, vol. 44, no. 6, pp. 1906–1913, Dec. 1997.

[37] S. N. Rashkeev, D. M. Fleetwood, R. D. Schrimpf, and S. T. Pantelides, "Proton-Induced defect generation at the Si-SiO_2 interface," *IEEE Trans. Nucl. Sci.*, vol. 48, no. 6, pp. 2086–2092, Dec. 2001.

[38] P. E. Bunson, M. D. Ventra, S. T. Pantelides, R. D. Schrimpf, and K. F. Galloway, "*Ab initio* calculations of H^+ energetics in SiO_2: Implications for transport," *IEEE Trans. Nucl. Sci.*, vol. 46, no. 6, pp. 1568–1573, Dec. 1999.

[39] S. T. Pantelides, S. N. Rashkeev, R. Buczko, D. M. Fleetwood, and R. D. Schrimpf, "Reactions of hydrogen with Si-SiO_2 interfaces," *IEEE Trans. Nucl. Sci.*, vol. 47, no. 6, pp. 2262–2268, Dec. 2000.

[40] S. N. Rashkeev, D. M. Fleetwood, R. D. Schrimpf, and S. T. Pantelides, "Defect generation by hydrogen at the Si-SiO_2 interface," *Phys. Rev. Lett.*, vol. 87, pp. 165506.1–165506.4, 2001.

[41] M. C. Payne, M. P. Teter, D. C. Allan, T. A. Arias, and J. D. Joannopoulos, "Iterative minimization techniques for Ab initio total-energy calculations: Molecular dynamics and conjugate gradients," *Rev. Mod. Phys.*, vol. 64, pp. 1045–1097, 1992.

[42] W. E. Pickett, "Pseudopotential methods in condensed matter applications," *Comp. Phys. Rep.*, vol. 9, pp. 115–198, 1989.

[43] D. Vanderbilt, "Soft self-consistent pseudopotentials in a generalized eigenvalue formalism," *Phys. Rev.*, vol. B 41, p. 7892, 1990.

[44] N. S. Saks and D. B. Brown, "Interface trap formation via the two-stage H^+ process," *IEEE Trans. Nucl. Sci.*, vol. 36, no. 6, pp. 1848–1857, Dec. 1989.

[45] M. R. Shaneyfelt, J. R. Schwank, S. C. Witczak, D. M. Fleetwood, R. L. Pease, P. S. Winokur, L. C. Riewe, and G. L. Hash, "Thermal-stress effects and enhanced low dose rate sensitivity in linear bipolar ICs," *IEEE Trans. Nucl. Sci.*, vol. 47, no. 6, pp. 2539–2545, Dec. 2000.

[46] M. P. Rodgers, D. M. Fleetwood, R. D. Schrimpf, I. G. Batyrev, S. Wang, and S. T. Pantelides, "The effects of aging on MOS irradiation and annealing response," *IEEE Trans. Nucl. Sci.*, vol. 52, no. 6, pp. 2642–2648, Dec. 2005.

[47] M. R. Shaneyfelt, R. L. Pease, J. R. Schwank, M. C. Maher, G. L. Hash, D. M. Fleetwood, P. E. Dodd, C. A. Reber, S. C. Witczak, L. C. Riewe, H. P. Hjalmarson, J. C. Banks, B. L. Doyle, and J. A. Knapp, "Impact of passivation layers on enhanced low-dose-rate sensitivity and pre-irradiation elevated-temperature stress effects in bipolar linear ICs," *IEEE Trans. Nucl. Sci.*, vol. 49, no. 6, pp. 3171–3179, Dec. 2002.

[48] I. G. Batyrev, M. P. Rodgers, D. M. Fleetwood, R. D. Schrimpf, and S. T. Pantelides, "Effects of water on the aging and radiation response of MOS devices," *IEEE Trans. Nucl. Sci.*, vol. 53, no. 6, pp. 3629–3635, Dec. 2006.

[49] K. M. Warren, R. A. Weller, M. H. Mendenhall, R. A. Reed, D. R. Ball, C. L. Howe, B. D. Olson, M. L. Alles, L. W. Massengill, R. D. Schrimpf, N. F. Haddad, S. E. Doyle, D. McMorrow, J. S. Melinger, and W. T. Lotshaw, "The contributions of nuclear reactions to heavy ion single event upset cross-section measurements in a high-density SEU hardened SRAM," *IEEE Trans. Nucl. Sci.*, vol. 52, no. 6, pp. 2125–2131, Dec. 2005.

[50] R. Baumann, T. Hossain, S. Murata, and H. Kitagawa, "Boron compounds as a dominant source of alpha particles in semiconductor devices," in *Proc. IEEE Int. Rel. Phys. Symp.*, 1995, pp. 297–302.

[51] R. Baumann, T. Hossain, E. Smith, S. Murata, and H. Kitagawa, "Boron as a primary source of radiation in high density DRAMs," in *Proc. Symp. VLSI Technol. Dig. Tech. Papers*, 1995, pp. 81–82.

[52] R. C. Baumann, "Soft errors in advanced semiconductor devices-part I: The three radiation sources," *IEEE Trans. Dev. Mater. Rel.*, vol. 1, no. 1, pp. 17–22, Mar. 2001.

[53] R. C. Baumann, "Radiation-Induced soft errors in advanced semiconductor technologies," *IEEE Trans. Dev. Mater. Rel.*, vol. 5, no. 3, pp. 305–316, Sep. 2005.

[54] R. C. Baumann and E. B. Smith, "Neutron-Induced boron fission as a major source of soft errors in deep submicron SRAM devices," in *Proc. IEEE Int. Rel. Phys. Symp.*, 2000, pp. 152–157.

[55] T. Calin, M. Nicolaidis, and R. Velazco, "Upset hardened memory design for submicron CMOS technology," *IEEE Trans. Nucl. Sci.*, vol. 43, no. 6, pp. 2874–2878, Dec. 1996.

[56] W. Shockley, "Problems related to P-N junctions in silicon," *Solid-State Electron.*, vol. 2, pp. 35–67, 1961.

[57] J. M. Benedetto and H. E. Boesch Jr., "The relationship between Co-60 and 10-keV x-Ray damage in MOS devices," *IEEE Trans. Nucl. Sci.*, vol. NS-33, no. 6, pp. 1318–1323, Dec. 1986.

[58] R. D. Schrimpf, R. A. Weller, M. H. Mendenhall, R. A. Reed, and L. W. Massengill, "Physical mechanisms of single-event effects in advanced microelectronics," *Nucl. Instrum. Meth. B*, vol. 261, pp. 1133–1136, 2007.

[59] A. S. Kobayashi, A. L. Sternberg, L. W. Massengill, R. D. Schrimpf, and R. A. Weller, "Spatial and temporal characteristics of energy deposition by protons and alpha particles in silicon," *IEEE Trans. Nucl. Sci.*, vol. 51, no. 6, pp. 3312–3317, Dec. 2004.

[60] A. S. Kobayashi, D. R. Ball, K. M. Warren, R. A. Reed, N. Haddad, M. H. Mendenhall, R. D. Schrimpf, and R. A. Weller, "The effect of metallization layers on single event susceptibility," *IEEE Trans. Nucl. Sci.*, vol. 52, no. 6, pp. 2189–2193, Dec. 2005.

[61] L. Scheick, "Microdose analysis of ion strikes on SRAM cells," *IEEE Trans. Nucl. Sci.*, vol. 50, no. 6, pp. 2399–2406, Dec. 2003.

[62] J. Allison, K. Amako, J. Apostolakis, H. Araujo, P. A. Dubois, M. Asai, G. Barrand, R. Capra, S. Chauvie, R. Chytracek, G. A. P. Cirrone, G. Cooperman, G. Cosmo, G. Cuttone, G. G. Daquino, M. Donszelmann, M. Dressel, G. Folger, F. Foppiano, J. Generowicz, V. Grichine, S. Guatelli, P. Gumplinger, A. Heikkinen, I. Hrivnacova, A. Howard, S. Incerti, V. Ivanchenko, T. Johnson, F. Jones, T. Koi, R. Kokoulin, M. Kossov, H. Kurashige, V. Lara, S. Larsson, F. Lei, O. Link, F. Longo, M. Maire, A. Mantero, B. Mascialino, I. McLaren, P. M. Lorenzo, K. Minamimoto, K. Murakami, P. Nieminen, L. Pandola, S. Parlati, L. Peralta, J. Perl, A. Pfeiffer, M. G. Pia, A. Ribon, P. Rodrigues, G. Russo, S. Sadilov, G. Santin, T. Sasaki, D. Smith, N. Starkov, S. Tanaka, E. Tcherniaev, B. Tome, A. Trindade, P. Truscott, L. Urban, M. Verderi, A. Walkden, J. P. Wellisch, D. C. Williams, D. Wright, and H. Yoshida, "Geant4 developments and applications," *IEEE Trans. Nucl. Sci.*, vol. 53, no. 1, pp. 270–278, Feb. 2006.

[63] M. H. Mendenhall and R. A. Weller, "An algorithm for computing screened Coulomb scattering in Geant4," *Nucl. Instr. Meth. B*, vol. 227, pp. 420–430, 2005.

[64] R. A. Reed, R. A. Weller, R. D. Schrimpf, M. H. Mendenhall, K. M. Warren, and L. W. Massengill, "Implications of nuclear reactions for single event effects test methods and analysis," *IEEE Trans. Nucl. Sci.*, vol. 53, no. 6, pp. 3356–3362, Dec. 2006.

[65] D. Ball, K. Warren, R. Weller, R. Reed, L. Massengill, R. Schrimpf, and N. Haddad, "Simulating nuclear events in a TCAD model of a high-density SEU hardened SRAM technology," in *Proc. RADECS*, Cap d'Agde, France, 2005.

[66] D. McMorrow, W. Lotshaw, J. Melinger, S. Buchner, Y. Boulghassoul, L. Massengill, and R. Pease, "Three-dimensional mapping of single-event effects using two photon absorption," *IEEE Trans. Nucl. Sci.*, vol. 50, no. 6, pp. 2199–2207, Dec. 2003.

[67] D. McMorrow, W. Lotshaw, J. Melinger, S. Buchner, and R. Pease, "Sub-bandgap laser-induced single event effects: Carrier generation via two-photon absorption," *IEEE Trans. Nucl. Sci.*, vol. 49, no. 6, pp. 3002–3008, Dec. 2002.

[68] K. M. Warren, B. D. Sierawski, R. A. Weller, R. A. Reed, M. H. Mendenhall, J. A. Pellish, R. D. Schrimpf, L. W. Massengill, M. E. Porter, and J. D. Wilkinson, "Predicting thermal neutron-induced soft errors in static memories using TCAD and physics-based Monte Carlo simulation tools," *IEEE Electron Dev. Lett.*, vol. 28, no. 2, pp. 180–182, Feb. 2007.

[69] K. M. Warren, B. D. Sierawski, R. A. Reed, R. A. Weller, C. Carmichael, A. Lesea, M. H. Mendenhall, P. E. Dodd, R. D. Schrimpf, L. W. Massengill, T. Hoang, H. Wan, J. L. De Jong, R. Padovani, and J. J. Fabula, "Monte-Carlo based on-orbit single event upset rate prediction for a radiation hardened by design latch," *IEEE Trans. Nucl. Sci.*, vol. 54, no. 6, pp. 2419–2425, Dec. 2007.

[70] A. D. Tipton, J. A. Pellish, R. A. Reed, R. D. Schrimpf, R. A. Weller, M. H. Mendenhall, B. Sierawski, A. K. Sutton, R. M. Diestelhorst, G. Espinel, J. D. Cressler, P. W. Marshall, and G. Vizkelethy, "Multiple-bit upset in 130 nm CMOS technology," *IEEE Trans. Nucl. Sci.*, vol. 53, no. 6, pp. 3259–3264, Dec. 2006.

[71] R. A. Reed, R. A. Weller, M. H. Mendenhall, J. M. Lauenstein, K. M. Warren, J. A. Pellish, R. D. Schrimpf, B. D. Sierawski, L. W. Massengill, P. E. Dodd, M. R. Shaneyfelt, J. A. Felix, J. R. Schwank, N. F. Haddad, R. K. Lawrence, J. H. Bowman, and R. Conde, "Impact of ion energy and species on single event effects analysis," *IEEE Trans. Nucl. Sci.*, vol. 54, no. 6, pp. 2312–2321, Dec. 2007.